Turkish Journal of Engineering
https://dergipark.org.tr/en/pub/tuje
e-ISSN 2587-1366

Evaluation of Removal Multi-Story Low-Rise RC Frame Demolition Using the Applied Element Method with Sequential Column Removal

M. Nadir Olabi[*1]

[1]*Bolu Abant Izzet Baysal University, Department of Building Information, Faculty of Architecture, Türkiye, nadirolabi@ibu.edu.tr*

Cite this study: Olabi, M. N. (2025). Evaluation of Multi-Story Low-Rise RC Frame Demolition Using the Applied Element Method with Sequential Column Removal. Turkish Journal of Engineering, 9 (2), 222-236.

https://doi.org/10.31127/tuje.1536922

Keywords
Applied Element Method
Progressive collapse
RC buildings
Demolition
Debris field

Research Article

Received:21.08.2024
Revised:13.11.2024
Accepted:18.11.2024
Published:01.04.2024

Abstract

Old reinforced concrete buildings are often beyond repair but occupy valuable land that could be used for modern, earthquake-resistant structures. The Applied Element Method (AEM) is a numerical analysis method used in building demolition analysis by dividing buildings into small elements connected by springs, allowing for comprehensive structural analysis under extreme loads. This study uses AEM to simulate the progressive collapse of low-rise 2D framed buildings by removing load-bearing elements sequentially from the first floor, observing collapse patterns, and analyzing debris field lengths (DF). The results show a consistent relationship between the debris field length (DF) and the building dimensions, particularly that DF could be calculated as the sum of the total length and height of the building, ensuring a reliable minimum safety margin for demolition design. Additionally, a multi-linear regression analysis is conducted to develop a accounting for the combined effects of various building characteristics, resulting in an equation for the minimum debris field length. Alternative demolition methods using tension cables to direct the collapse debris to one side were also explored, demonstrating significant DF reductions compared to standard approaches. These results highlight the importance of examining controlled demolition strategies, that enhance safety margins and ensure predictable demolition outcomes.

1. Introduction

The recent advancements in building construction and design methods, based on modern building standards, have enabled the construction of reinforced concrete (RC) structures with high specifications and better utilization of spaces [1-3]. This progress has drawn attention to old and existing buildings constructed with outdated design codes and poor-quality materials, highlighting the need to either strengthen or remove these structures [4, 5]. Additionally, these buildings were not designed to withstand forces such as lateral loads, which were not adequately considered in the traditional construction methods of their time. Furthermore, many of these structures have been exposed to weather and environmental factors for extended periods, further weakening them and increasing their wear. As a result, costly and labor-intensive repairs have become necessary. Therefore, it is crucial to study the methods and procedures for removing these buildings to reuse the spaces they occupy, especially in city centers, for the construction of modern buildings with greater efficiency and improved resistance to natural forces, such as seismic events. However, traditional methods for building removal, such as using hand-held and lightweight machinery like compressors and hammers, or heavyweight machines like wrecking balls and excavators, are considered high-cost due to the extensive equipment and manpower required. These methods are also unsafe, particularly regarding the scattered and falling debris during the removal operation. Therefore, it is necessary to investigate new and scientific methods that are faster and more cost-efficient compared to traditional methods for removing and demolishing reinforced concrete (RC) buildings [6].

According to the American Society of Civil Engineers [7], progressive collapse refers to the gradual spread of a local structural element failure to other structural elements, ultimately resulting in the collapse of the entire structure or a significant portion of it. Many researchers have conducted extensive studies, both experimental and numerical, focusing on the mechanisms and design of

progressive collapse due to its increasing importance over the last 20 years [8-11]. Since experimental studies on progressive collapse are very expensive, difficult, and, most importantly, risky, many researchers prefer numerical methodologies [12, 13]. Published studies use three main types of analysis methods: the Finite Element Method (FEM), the Discrete Element Method (DEM), and the Applied Element Method (AEM). For instance, Kabele et al. [14] conducted a demolition simulation on a multi-story precast building using the FEM-based commercial code ATENA. Similarly, Zhang et al. [15] proposed analytical and numerical models to assess progressive collapse, with the numerical model utilizing the FEM platform OpenSees [16]. Other examples of FEM-based analysis can be found in the literature using well-known packages such as ABAQUS, LS-DYNA, and SAP2000 [14, 17]. Although the Finite Element Method has shown good performance in reproducing RC structure collapses, the number of simplifications and modifications required for FEM progressive collapse simulations can be extensive, to the point where analysis might be impractical in some situations [14, 17]. Likewise, DEM is rarely used for simulations due to its time-consuming nature, the need for very detailed models, and its lower accuracy compared to FEM. The Applied Element Method, on the other hand, has demonstrated similar capabilities to FEM but requires fewer modifications, allowing for full 3D progressive collapse simulations within a reasonable timescale [18]. Many studies have utilized the AEM for progressive collapse assessment and demolition simulations involving various RC elements [19-21], primarily using the Extreme Loading for Structures (ELS) software [22]. The evaluation of AEM will be discussed later in this paper.

The main aim of this study is to determine the actual collapse patterns of low-rise framed reinforced concrete buildings by dismantling load-bearing columns to initiate a progressive collapse for the purpose of removing the entire building. Additionally, the financial and safety aspects of the removal process are considered by minimizing the number of columns removed to reduce costs and potential damage to surrounding neighborhoods. To achieve these goals, a nonlinear dynamic analysis is performed using numerical models developed with the Applied Element Method, allowing for the observation of all collapse stages. A prototypical four-story RC building is designed according to old standards to represent existing buildings or those intended for removal due to inefficiency. Various characteristics of this building are used as study parameters to produce 21 different models with a range of properties that reflect real buildings found in countries like Syria and Türkiye.

2. Applied Element Method

The Applied Element Method (AEM) is a discrete element numerical analysis method that combines the advantages of Finite Element Methods (FEM) with the benefits of Discrete Element Methods (DEM). AEM offers simplicity in modeling with highly accurate results and requires less computing time compared to other analysis methods [23]. AEM uses a modeling approach that allows for tracking the full behavior of the structure through different loading phases, from the elastic stage to crack onset and propagation, reinforcement yielding, nonlinear deformations, element separation and rigid body motions, recontacting, and collision of separated elements, ultimately leading to full collapse and impact with the ground. AEM discretizes the structure into small elements connected by a set of normal and shear springs at each contact point on the faces of the elements (Figure 1). At each contact point in a full 3D model, three springs are formed, one normal and two shear springs, which represent the material properties at that point. For instance, Figure 1 shows a reinforced concrete (RC) element where concrete and steel are represented separately through their corresponding sets of springs. This configuration allows for easy consideration of reinforcement details, as steel springs can be placed according to the exact locations of the real steel bars for both longitudinal and transverse reinforcement.

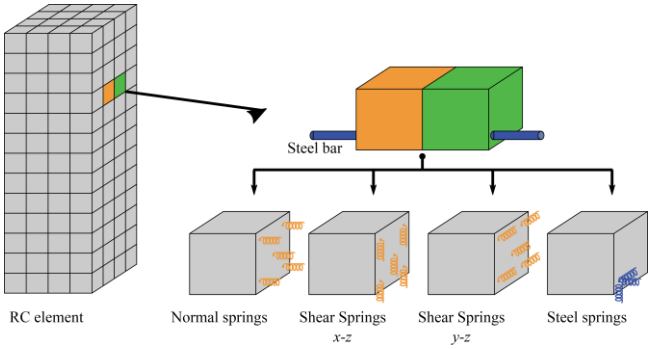

Figure 1. Element connectivity with springs in AEM

2.1. AEM formulation

As mentioned before, structures in AEM are divided into virtual small elements connected by a matrix of springs. Each spring determines the stress, strain, and deformations of the surrounding area. The normal and shear springs in Figure 2 represent the material properties of the two discrete elements, and the stiffness of the springs is calculated as seen in Equations 1 and 2.

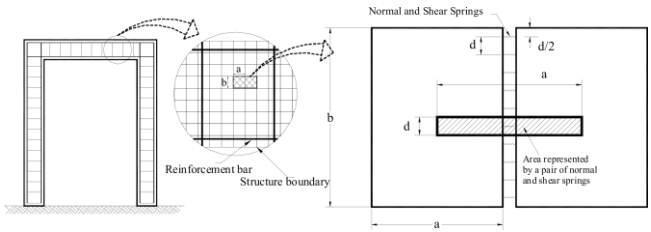

Figure 2. Element formulation and spring distribution in planar AEM model [23]

$$K_n = \frac{E.d.t}{a} \quad (1)$$

$$K_s = \frac{G.d.t}{a} \quad (2)$$

In the equations, K_n and K_s are the stiffness of the normal and shear springs, respectively, a is the element length, t is the element thickness, d is the distance

between the springs, and E and G are Young's modulus and the shear modulus of the material, respectively. For RC elements, dt in this equation represents the concrete area, but for steel reinforcement, this area is replaced with the area of the corresponding bar. Moreover, by applying a unit displacement and calculating the force at the center of elements, the resulting element stiffness matrix will be of size 6 × 6 [20].

2.2. AEM evaluation

Extensive work across a wide range of applications has been performed to evaluate AEM and verify the accuracy of its results. The linear and nonlinear simulation performance of the Applied Element Method was tested against monotonic experimental results and showed reliable agreement [23, 24]. Additionally, Meguro and Tagel-Din [25] conducted nonlinear cyclic numerical analyses to examine the failure behavior of reinforced concrete structures, including crack initiation, propagation, and opening and closing during each cycle. The study demonstrated that the model could follow the real structure's response without any predefined locations or spreading of the cracks. Furthermore, the size of the elements and the number of connecting springs were studied, revealing that using smaller elements with fewer springs (5 to 10 springs) provides optimal results in terms of error ratio and CPU time [24]. Consequently, using special terms added to the stiffness matrix, Poisson's ratio could be integrated without increasing the processing time of the analysis.

Moreover, an extension for AEM was introduced to account for large displacements in static and dynamic loading scenarios, and the results proved the method's ability to analyze structures in these extreme ranges [26-28]. Sasani [29] evaluated the collapse of the six-story Hotel San Diego with infills after the removal of load-bearing exterior columns. Griffin [30] conducted a comparison study using the software Extreme Loading for Structures (ELS) and simulated two actual building demolition projects to examine the progressive collapse predictability of the Applied Element Method. Lupoae and Bucur [31] compared an AEM numerical model of an RC structure with load-bearing walls and columns to the real demolition of the building. These researchers demonstrated that the program ELS and AEM are capable of accurately following the local and global collapse stages and modeling the debris field of reinforced concrete structures. Additionally, Alhafian [17] conducted an experimental and analytical study on three RC structures tested using a shaking-table experiment. The numerical models showed a good degree of agreement with the experimental results, demonstrating the reliable performance of AEM in predicting the total response of structures under seismic loads, from the elastic stage to the full collapse of the structure.

3. Model Development and Validation

In the scope of this study, numerical models are developed using the software Extreme Loading for Structures [22] version 2.3. This program relies on the Applied Element Method as the theoretical structural analysis procedure. Initially, a numerical model was built using parameters recommended by various researchers in the literature [17, 30]. The simulation was validated against the behavior of an experimentally tested RC frame under lateral loads [32]. Subsequently, the validated numerical model with the calibrated parameters was used to conduct the building removal parametric investigation.

3.1. Material models in ELS

The compressive concrete material model adopted in ELS is the Maekawa model [33]. This nonlinear model is assigned to concrete normal springs, seen in Figure 1, to represent the compression behavior defined by the Young's modulus E, compressive strength f_c, and the corresponding compressive strain ε_p. For the tension response, the adopted model uses linear stiffness up to the maximum tensile strength and drops to zero after that (Figure 3a). On the other hand, shear springs representing the shear behavior of concrete are modeled using the stress-strain relationship shown in Figure 3b. In this model, the shear stress maintains a constant value after dropping from the cracking strength to accommodate the interlocking and friction effects [22]. Additionally, Figure 3c shows the steel model used in ELS and in this study. The laws presented by Ristic et al. [34] are applied to the steel springs to account for the nonlinear response, including the loading and unloading history and the Bauschinger effect. This model has bi-linear branches, where the post-yield stiffness is taken as 1% from the initial stiffness E_s.

3.2. Contact and separation parameters in ELS

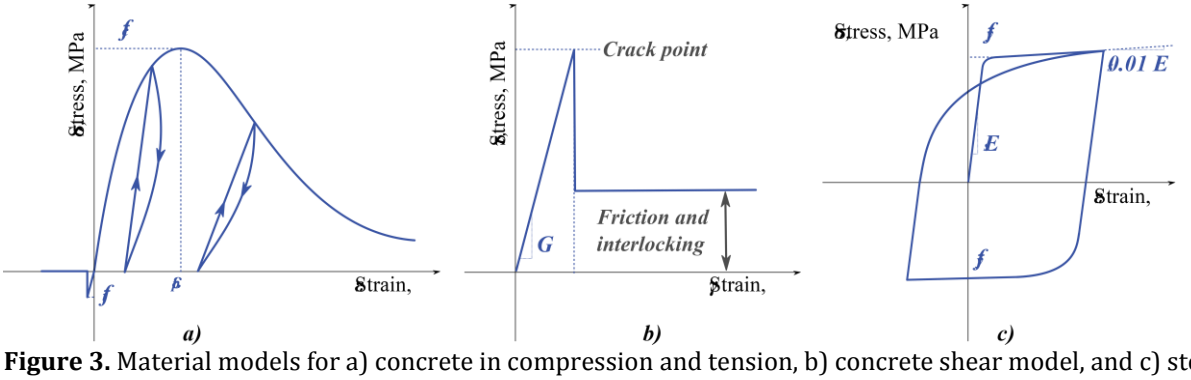

Figure 3. Material models for a) concrete in compression and tension, b) concrete shear model, and c) steel model

One of the most important features of AEM is its ability to separate elements after failure and track their collision and recontact during the demolition of the structure. This capability is also useful in the nonlinear stages before failure, where the opening and closing of cracks are determined through the separation strain ε_{sep}, and the contact parameters. Separation strain is defined as the strain at which two opposite elements are considered fully separated and treated as completely different elements by AEM. Separation strain effects act only on concrete springs, so when the predetermined value is reached, all the springs connecting the two elements, including steel springs, will be cut. Moreover, if the two elements recontact, the model will form two contact springs, normal and shear, between them to simulate the collision behavior. The stiffness characteristics of these springs are determined by the Normal Contact Stiffness Factor (NF) and the Shear Contact Stiffness Factor (SF) for the normal and shear springs, respectively. Equations 3 and 4 show the normal and shear stiffnesses k_1 and k_2, respectively, for the newly created contact springs, where E is the minimum stiffness of the two elements, and D is the centroid distance.

$$k_1 = E.NF.D \quad (3)$$

$$k_2 = E.SF.D \quad (4)$$

Furthermore, since energy is dissipated during collision events, the Contact Spring Unloading Stiffness Factor (n) accounts for this energy reduction by modifying the unloading stiffness of the contact springs by n, corresponding to an energy decrease equal to $1 - 1/n$. According to evaluation studies conducted by previous researchers such as Alhafian [17] and Griffin [30], while the separation strain value should be chosen to be higher than the ultimate tensile strain of the reinforcing steel to prevent untenable failures, the values of the other parameters adopted in this paper are demonstrated in Table 1.

Table 1. Contact and separation parameters adopted for the ELS software

NF	***SF***	***n***
0.0001	0.00001	2

3.3. Numerical model validation

A numerical model is developed using ELS and AEM, utilizing the previously discussed material models and analysis parameters. To evaluate this model, a comparison study is conducted against existing experimental work, where a reinforced concrete frame is tested under lateral loading [24, 32]. The frame has very conventional steel detailing and could be a good representation of old and existing RC buildings. By comparing the results presented in Figure 4, the numerical and experimental curves show very good agreement, and the ELS model from the current study is comparable to previous works [24]. As seen from the figure, small differences appeared at the final stages of loading with approximately 5% error ratios. These results show the excellent ability of the Applied Element Method and ELS software to simulate the response of RC frames.

4. RC frames demolition parametric study

The parametric investigative study begins with choosing and designing a prototype frame structure representing old buildings in removal projects. Following this, a set of 21 models is produced by varying the concrete quality f_c, reinforcement ratio ρ, stirrup density, and beam span b (Figure 5 and Table 2). Subsequently, load-bearing elements (columns) are removed from the first floor to initiate a progressive collapse and achieve a fully demolished building ready for removal.

4.1. Design of the prototype RC frame

To comply with the objective of the study, a prototype RC building with a frame structural system was designed to withstand vertical loads only, as commonly seen in old and existing buildings, which are the target of this work. The reference frame, named E1 and shown in Figure 5.a, has four typical floors with a level height $h = 3.5\ m$.

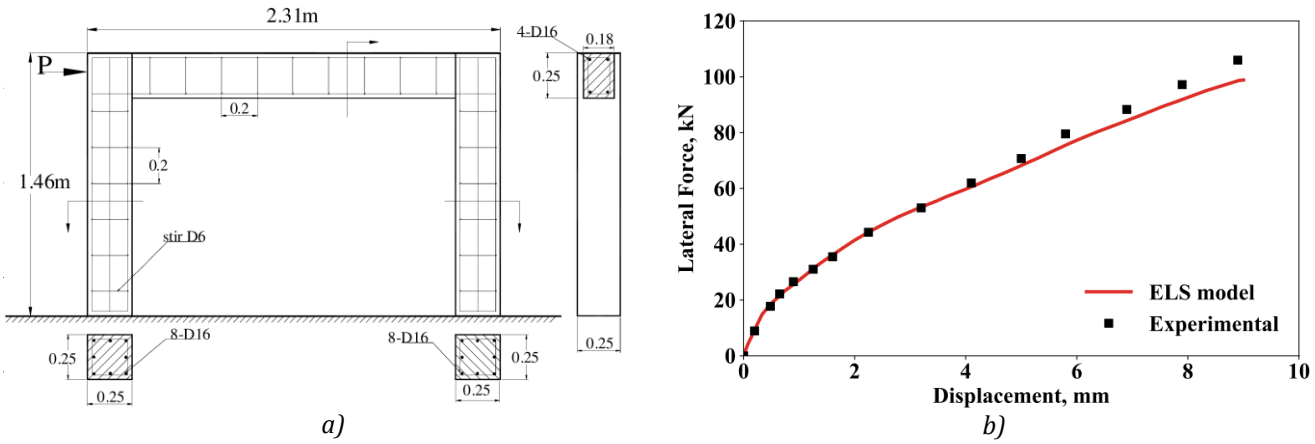

a) *b)*

Figure 4. a) Geometry of experimentally tested frame from [32], and b) Comparison of experimental and numerical results using ELS

Table 2. Characteristics of the 21 RC frame numerical models used in the study

Model No. / Transverse reinforcement			b (m)	ρ (%)	f_c (MPa)
Light	Moderate	Dense			
E1	E2	E3	4.0	1.0	18.0
E4	E5	E6	3.0		
E7	E8	E9	5.0		
E10	E11	E12	4.0	0.7	
E13	E14	E15		1.4	
E16	E17	E18		1.0	12.0
E19	E20	E21			25.0

Three frame openings were adopted for the prototype building, with a beam span $b = 4\ m$ for the reference E1. The reference frame was designed based on older standards [35] with simple calculation methods to determine the dimensions of the structural elements and their reinforcement. Columns and beams dimensions and steel detailing are presented in Figure 5.a, where the yield strength of the steel is $f_y = 240\ MPa$ and the concrete strength for the base model E1 is $f_c = 18\ MPa$.

4.2. Characteristics and parameters of the RC frame models

Table 2 shows the different characteristics of the 21 models produced by varying concrete quality, steel ratio, transverse reinforcement density, and beam span. All parameters were determined by reducing or increasing the base values by approximately 0.7 and 1.4, respectively. For instance, the reinforcement ratios were chosen as *0.7%*, *1.0%*, and *1.4%* for the longitudinal steel in columns, and similarly, the ratio in the beam was varied based on the same proportions. Moreover, concrete strength was selected as *12*, *18*, and *25 MPa*, reflecting common values found in old buildings. The beam span was assigned as 3, 4, and 5 meters. Additionally, three types of transverse reinforcement were defined for both columns and beams to investigate their effect on the collapse shape and the final demolished building debris field (DF). Light, moderate, and dense ratios were selected as $\phi 8/250$, $\phi 10/170$, and $\phi 10/100$, respectively. These steel details were applied to a quarter of the length of the elements at each end, while the middle section retained the lighter transverse reinforcement ratios (Figure 5). Additionally, the transverse steel did not extend into the joint, following common practices found in older buildings (Figure 5.b).

4.3. Model parameters in ELS

Accurate and efficient modeling of the RC structure in the ELS program requires careful selection of various parameters and specifications. The model elements are divided into finite applied elements with a mesh size of approximately $10 \times 10\ cm$ for beams and columns, and $5 \times 5\ cm$ for joints. The smaller mesh size for the joints enhances the accuracy of stress and strain calculations and the formation of cracks within the joints. In addition, the choice of the number of springs connecting the faces of the applied elements depends on the required accuracy of the study and is balanced with the analysis speed. According to reference studies and theoretical considerations [23], the effect of the number of springs diminishes as the size of the applied element decreases relative to the structure's size. Since the chosen mesh is relatively small, reducing the number of springs does not significantly affect accuracy. Nevertheless, it was decided to use 5 springs per face to ensure precision. Also, the contact parameters determine the stiffness of the springs formed at the contact or collision between two elements. These factors are derived from previous studies [17, 30], as outlined in Table 1. Moreover, Tables 3 and 4 demonstrate the specifications adopted for concrete and reinforcing steel used in the models, respectively.

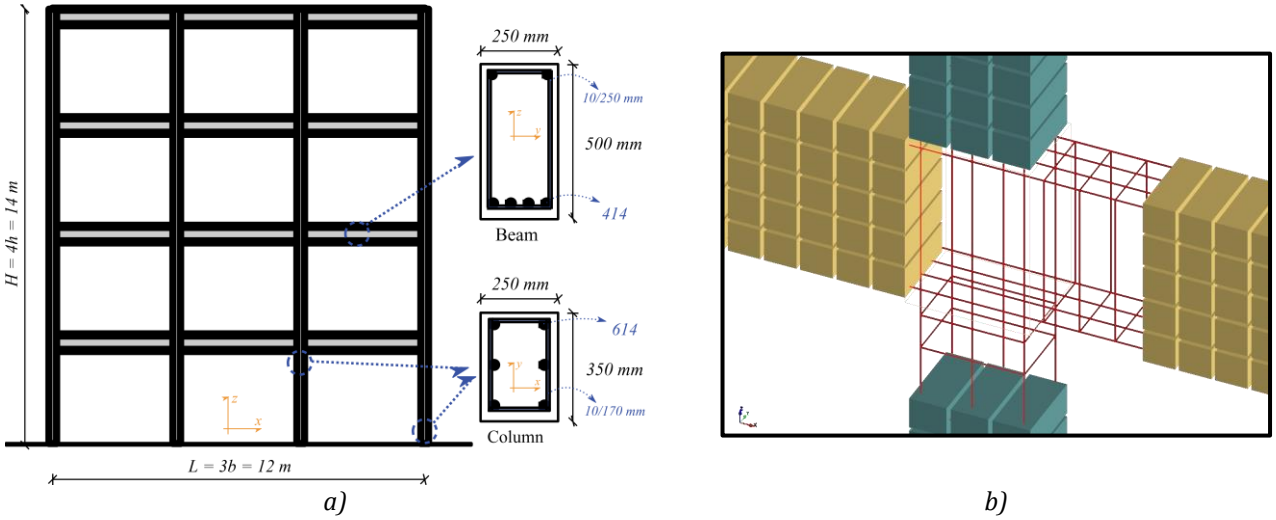

Figure 5. a) The reference prototype numerical frame, E1, of the RC frames used in the modeling and removal study, and b) a screenshot from ELS showing steel detailing and element division at beam-column joints

Table 3. Concrete characteristics used in the numerical model

f_c (MPa)	E (MPa)	G (MPa)	Specific weight (t/m^3)	ε_{sep}
12	16281.3	4884.4	2.5	0.1
18	19940.4	5982.1	2.5	0.1
25	23500.0	7050.0	2.5	0.1

Table 4. Steel characteristics used in the numerical model

f_y (MPa)	E_s (MPa)	G (MPa)	Specific weight (t/m^3)	ε_{sep}
240	200e3	80e3	7.84	0.2

Modules of elasticity and shear modulus for the concrete were calculated as in Equations 5 and 6.

$$E = 4700\sqrt{f_c} \quad (5)$$

$$G = 0.3E \quad (6)$$

4.4. Loading scenarios

To accurately represent the entire process of the structure, including the application of vertical loads, the removal phase, and the subsequent collapse, the analysis is conducted in two stages. In the first stage, known as static analysis, only vertical loads represented by the self-weight of the structure are applied. Additional loads, whether dead or live, are not considered since the scenario involves removing all contents from the building in order to prepare it for the demolition work, leaving only the load bearing frames. The second stage involves dynamic analysis, focusing on the removal of structural elements and the resulting collapse. For this stage, two values must be determined. The first is the analysis duration, which must be long enough to allow the collapse to occur and all parts of the structure to stabilize in their final state. The second value is the time step which significantly impacts the accuracy of results regarding displacements, deformations, and collisions between elements. While reducing the time step increases the analysis time considerably, a larger time step results in less accurate outcomes. The optimal time step for dynamic analysis is influenced by the mass of the elements and the stiffness of their connections. When the mass is relatively large, like in reinforced concrete structures, longer time steps are acceptable and typically range between 0.001 and 0.01 seconds [22]. It is important to note that although a smaller time step is generally preferred for analyzing the detailed behavior of the structural elements, this study used a relatively larger time step of 0.01 seconds. This choice was made to balance analysis time while still providing an adequate representation of the overall collapse, structural damage, and the resulting condition of the debris pile.

4.5. Column removal sequences

The most effective and straightforward method for demolishing a structure involves removing all load-bearing elements, mainly columns, on each floor. However, this approach presents several significant issues including the need for extensive removal work and significant amounts of explosive material if blasting is employed, leading to high costs. Additionally, the removal process generates a large pressure wave that can be damaging to the surrounding environment and adjacent structures and creates substantial quantities of small debris that hat can scatter uncontrollably. For those reasons, this study proposes an alternative approach by selectively removing a small set of columns to initiate a progressive collapse of the building, ultimately aiming for a stable state of complete collapse. The demolition process will begin with the removal of non-load-bearing elements, such as windows, doors, mechanical fixtures, and other non-structural components, while retaining only the RC frames. This initial step ensures that these non-structural elements do not impede the collapse process due to their unaccounted load-bearing capacities. Following this, a limited number of load-bearing elements (columns) will be removed to induce a progressive collapse of the structure. Once the collapse is initiated, the resulting debris will be cleared using conventional methods, including heavy machinery such as crushers and bulldozers.

Additionally, this work employs a demolition method where columns are removed from one side of the building. This side is chosen as the direction in which the collapse is intended to occur, thereby directing most of the debris in that direction. This demolition method was selected based on experiments with various demolition procedures demonstrating that removing columns from floors other than the ground floor was ineffective in modifying the size or direction of the debris pile. Consequently, for optimal results with only the columns on the ground floor will be removed as seen in Figure 6.

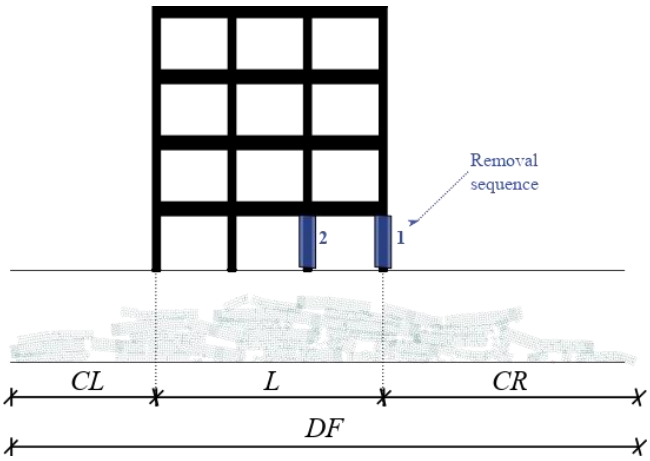

Figure 6. Element removal procedure conducted in this work

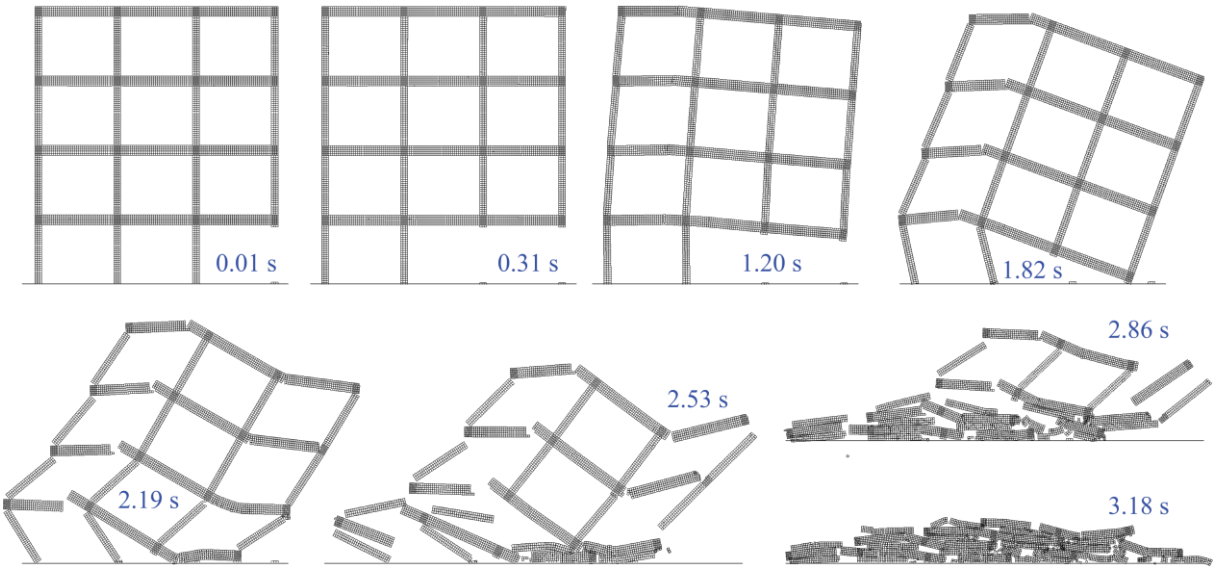

Figure 7. Mechanism and progressive collapse form for frame E1

The numbers shown in Figure 6 indicate the sequence for removing each column. Sequential removal is essential to induce the necessary degradation and formation of cracks and plastic hinges to achieve the desired collapse pattern. Consequently, it is crucial to determine the time interval between the removal of each set of elements [7]. According to Kabele et al. [14], using intervals of less than 300 milliseconds between the removal of elements is ineffective and does not allow for the desired collapse. This is because the time required for the structure to begin moving after the removal of initial elements is at least 50 to 100 milliseconds. If the interval is less than 300 milliseconds, the elements remain interconnected and continue to bear the moments transferred between them. On the other hand, longer intervals promote the deterioration of connections between beams and columns, providing sufficient time for plastic hinges to form. Therefore, in this study a time interval of 300 milliseconds was chosen between the removal of each ground floor column.

5. Results and Discussion

The analysis is applied to all selected E frame models, as shown in Table 2, totaling 21 numerical analyses. For example, Figure 7 illustrates the stages of the progressive collapse for the model E1, which serves as the reference model designed as an example of a current condition case. The collapse stages are indicated in the figure with specific times, showing the removal of the first column at 0.01 seconds, followed by the removal of the second column after 300 milliseconds at 0.31 seconds. Subsequently, the formation of plastic hinges begins at

Table 5. Measurements of the debris field for all E models following the collapse analysis (mm)

Model No.	L	CL	CR	DF	DF/L	$DF/(L+H)$
E1	1200.0	364.0	1034.0	2,598.0	2.17	1.00
E2	1200.0	352.0	817.0	2,369.0	1.97	0.91
E3	1200.0	316.0	1029.0	2,545.0	2.12	0.98
E4	900.0	334.0	1073.0	2,307.0	2.56	1.00
E5	900.0	384.0	755.0	2,039.0	2.27	0.89
E6	900.0	354.0	953.0	2,207.0	2.45	0.96
E7	1500.0	537.0	1001.0	3,038.0	2.03	1.05
E8	1500.0	526.0	905.0	2,931.0	1.95	1.01
E9	1500.0	757.0	710.0	2,967.0	1.98	1.02
E10	1200.0	542.0	477.0	2,219.0	1.85	0.85
E11	1200.0	384.0	578.0	2,162.0	1.80	0.83
E12	1200.0	533.0	580.0	2,313.0	1.93	0.89
E13	1200.0	513.0	982.0	2,695.0	2.25	1.04
E14	1200.0	526.0	890.0	2,616.0	2.18	1.01
E15	1200.0	556.0	1000.0	2,756.0	2.30	1.06
E16	1200.0	466.0	683.0	2,349.0	1.96	0.90
E17	1200.0	714.0	747.0	2,661.0	2.22	1.02
E18	1200.0	568.0	965.0	2,733.0	2.28	1.05
E19	1200.0	374.0	1068.0	2,642.0	2.20	1.02
E20	1200.0	392.0	987.0	2,579.0	2.15	0.99
E21	1200.0	527.0	922.0	2,649.0	2.21	1.02
mean		477.10	864.57	2541.67	2.13	0.98
STD		121.20	177.21	275.50	0.19	0.07
COV		0.25	0.20	0.11	0.09	0.07

1.20 seconds, leading to the propagation of failed elements and initial contact of the structure with the ground at 1.82 seconds. Finally, the collapse stabilizes completely at 3.18 seconds. Additional examples of the progressive collapse sequence are provided in the appendix, moreover, all figures and details of the other E models are available from Olabi [36]. It is worth noting that collapse did not occur by removing a single column; however, all the models completely collapsed with the removal of two columns in the sequence shown in Figure 6, except for the models with a 3-meter frame span named E4, E5, and E6. For these models, the third ground-floor column had to be removed to achieve complete collapse. This adjustment was necessary because removing only two columns did not result in a collapse; the frame remained standing with significant deformations.

After conducting the analysis and allowing all debris to stabilize, the distances CR and CL are measured as shown in Figure 6. CR represents the distance from the structure's facade to the furthest stable debris piece on the side where the collapse was intended and where columns were removed (the right side in this study). Conversely, CL is the distance from the structure's facade to the furthest stable debris piece on the opposite side of the desired collapse direction (the left side in this study). Using these measurements, the total debris field (DF) width, which indicates the spread of debris post-collapse stabilization, can be calculated as $DF = CL + 3b + CR$. Table 5 provides the measurements of CR, CL, and DF for all E models. Accordingly, Figure 8 illustrates the changes in debris field variations with respect to span length, reinforcement ratio, and concrete strength, for each case of light, medium, and dense stirrups.

5.1. Impact of frame properties on DF

From Figure 8, the ratios of the derbies field (DF) to the sum of frame height and total width indicate that DF increases naturally with the span length. This is primarily due to the increase in L, as well as the length of the collapsed beams, which increases the debris spread and enlarges the resulting pile. Additionally, varying stirrup densities has an insignificant effect on the debris spread, with the largest difference observed in the smallest span (3 meters), measuring 268 cm, which is about 12.3% of the average DF value. This difference decreases with increasing span length, reaching around 3.5% of the average DF for the 5-meter span. Furthermore, there is no direct impact of transverse reinforcement density on the debris field, as the DF values overlap for each span length. Interestingly, the DF value for medium stirrup density is lower than that for both light and dense stirrups, a trend also seen when other characteristics are varied.

Moreover, it is observed that DF increases with the reinforcement ratio in both beams and columns. Various collapse patterns show that as the longitudinal reinforcement ratio increases, the beams, in particular, remain continuous and exhibit catenary action. This prevents interruptions during the collapse progression, pushing the debris further from the original boundaries of the structure. This specifically increases the CR value, thereby expanding the debris field (DF). Also, as mentioned before the impact of stirrup density is minimal and does not have a direct effect, as DF values for different stirrup densities overlap. The differences in DF for all transverse steel cases do not exceed 9% of the average DF value at each longitudinal reinforcement level.

The effect of transverse reinforcement (stirrups) appears to be more evident when varying the concrete strength, f_c. When the concrete strength is low, the transverse reinforcement acts as confinement for the concrete section, making the beams more cohesive and maintaining larger pieces during the collapse process. This causes the debris to be pushed further from the original structure boundaries, increasing the DF value. Conversely, less transverse reinforcement leads to fragmentation of the concrete sections, causing the collapse to occur closer to the structure's boundaries, thereby reducing the DF value. This effect diminishes as the concrete strength increases, as the concrete itself contributes more to resisting shear forces along with the transverse reinforcement. Thus, the impact of concrete on the debris field primarily depends on the shear reinforcement. When the concrete is weak, the shear reinforcement plays a significant and clear role. As the concrete strength increases, its reliance on shear reinforcement decreases.

5.2. Proposed debris field length equations

One of the key observations from Table 5 is the consistent relationship between the debris field (DF) and the total length of the building. Specifically, DF is shown

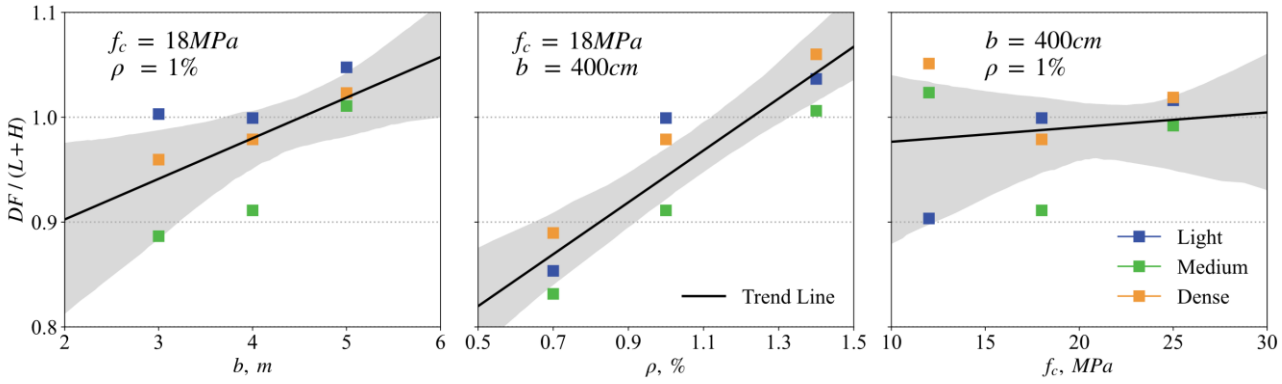

Figure 8. Debris field variations with different frame model characteristics, with trend line and 95% confidence interval.

to be approximately 2.13 times the length (L), with an error margin of about 9%. Furthermore, a more refined observation reveals that DF is roughly 0.98 times the sum of the length and height of the frame, with a smaller error margin (7%). This tighter correlation suggests that both the length and height of the building play significant roles in determining the extent of the debris spread. Consequently, for practical purposes, a simple and slightly conservative equation is proposed (Equation 7) to estimate the debris field, ensuring a reliable approximation for engineering applications.

$$DF = L + H \tag{7}$$

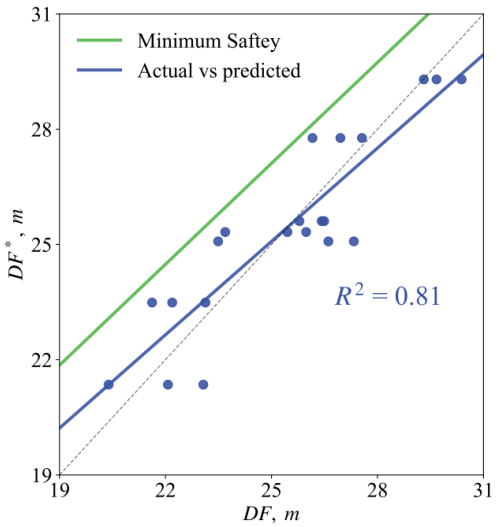

Figure 9. Actual debris field lengths compared to predicted values from the multi-linear regression model

In addition, to account for the effects of various frame characteristics (b, ρ, and f_c) presented in Figure 8 a multi-linear regression analysis was conducted to derive a more comprehensive relationship for DF, considering the combined effects of frame span (cm), reinforcement ratio (%), and concrete strength (MPa). The resulting equation, presented in Equation 8, achieved an R^2 value of 0.81, suggesting a robust model that accounts for multiple influencing factors. Figure 9 illustrates the correlation between the actual (DF) and predicted (DF*) values based on this multi-linear regression, highlighting the predictive capability of the derived equation. For safety considerations, the trend line from Figure 9 was adjusted upwards to include all data points, accounting for any potential errors. This conservative approach led to modification of Equation 8 and producing Equation 9, which calculates the minimum debris field length, DFL_m, thereby enhancing the safety margin in calculating and designing RC buildings demolition projects.

$$DF^* = 258.76 + 3.97b + 612\rho + 4.06f_c \tag{8}$$

$$DFL_m = 280 + 4.3b + 660\rho + 4.4f_c \tag{9}$$

5.3. One-sided collapse

The previous analysis of selected E frame models demonstrated that debris piles form on both sides of the structure when executing a typical column removal to generate progressive collapse. However, in many cases, it is necessary for the collapse to occur in a single direction due to the presence of neighboring structures, utility services, water channels, electrical and communication lines, or other installations. In these scenarios, it is essential to achieve $CL = 0$ and $DF = L + CR$. To obtain this result, a proposed method utilizing tension cables placed to pull the structure towards the desired direction of the debris during the collapse (Figure 10). Based on the results shown previously in Table 5 of the typical removal process, it has been found that tying at least two floors is necessary because the collapse can otherwise occur in the opposite direction, resulting in CL reaching up to two floor heights in some cases.

Some tests were conducted to place the tension cables in various points, but it was concluded that they should be connected directly to the ground, as seen in Figure 10. The other methods were unsuccessful in preventing debris formation on the left side. It was also noticed that the column ends were fragmenting, and parts were separating, freeing the cables and causing the columns to

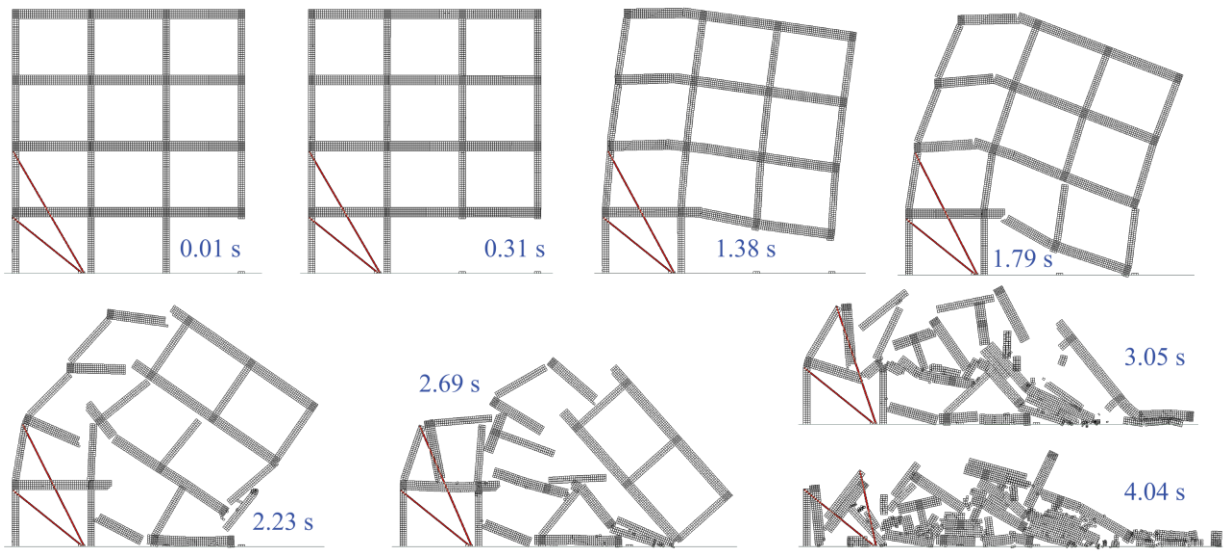

Figure 10. Mechanism and progressive collapse form for one-sided collapse scenario, frame E2

Table 7. Measurements of the debris field for the one-sided collapse scenario (mm)

Model No.	L	CL	CR	DF	DF/L	$DF/(L+H)$
E1	1200.0	0.0	1279.0	2479.0	2.17	1.00
E2	1200.0	0.0	1056.0	2256.0	1.97	0.91
E3	1200.0	0.0	1215.0	2415.0	2.12	0.98
E4	900.0	0.0	1314.0	2214.0	2.56	1.00
E5	900.0	0.0	1309.0	2209.0	2.27	0.89
E6	900.0	0.0	1264.0	2164.0	2.45	0.96
E7	1500.0	0.0	579.0	2079.0	2.03	1.05
E8	1500.0	0.0	576.0	2076.0	1.95	1.01
E9	1500.0	0.0	407.0	1907.0	1.98	1.02
E10	1200.0	0.0	713.0	1913.0	1.85	0.85
E11	1200.0	0.0	700.0	1900.0	1.80	0.83
E12	1200.0	0.0	779.0	1979.0	1.93	0.89
E13	1200.0	0.0	1439.0	2639.0	2.25	1.04
E14	1200.0	0.0	1361.0	2561.0	2.18	1.01
E15	1200.0	0.0	1521.0	2721.0	2.30	1.06
E16	1200.0	0.0	767.0	1967.0	1.96	0.90
E17	1200.0	0.0	1027.0	2227.0	2.22	1.02
E18	1200.0	0.0	942.0	2142.0	2.28	1.05
E19	1200.0	0.0	718.0	1918.0	2.20	1.02
E20	1200.0	0.0	701.0	1901.0	2.15	0.99
E21	1200.0	0.0	963.0	2163.0	2.21	1.02
		mean	982.38	2182.38	1.86	0.84
		STD	326.92	253.23	0.36	0.12
		COV	0.33	0.11	0.19	0.14

collapse in the unintended direction. Therefore, it is necessary to strengthen the column ends before conducting this proposed removal method. This was modeled in ELS by changing the material of the elements at the column heads where the cable is connected to steel elements with the same characteristics as the reinforcement steel. The tension cables were modeled using Link Members from the ELS library with specifications shown in Table 6. Strengthening the column ends ensured that the cables remained securely in place during the collapse, effectively directing the debris to the intended side.

Table 6. Specifications for the tension cables used in ELS model

Diameter (mm)	F_u (MPa)	E_s (MPa)	Specific weight (t/m^3)	ε_{sep}
25.4	620	200e3	7.84	0.1

As seen in Figure 10, the stages of progressive collapse for model E2 are presented with time steps of notable events during the progressive collapse. The measurements of CR, CL, and DF for all E models are detailed in Table 7. The table indicates a substantial reduction in DF values compared to those from the ordinary progressive collapse models, about 17% less in average values. The primary reason for these decreases is the restriction of debris spread by preventing collapse on the left side, resulting in a barrier formed by the column tied with the tension cable, which led to smaller dimensions of the debris pile.

Additionally, Figure 11 shows the variations in debris field with respect to span length, reinforcement ratio, and concrete strength for each case, considering light, medium, and dense stirrups. The figure indicates the limited impact of stirrup reinforcement density which remains evident in the case of total progressive collapse with tension cables. The overlap between the curves for each transverse reinforcement case shows no substantial differences in values for any span studied, with variations not exceeding 9% of the average DF value for each span. Unlike the ordinary progressive collapse scenario, DF does not increase for larger spans, as the

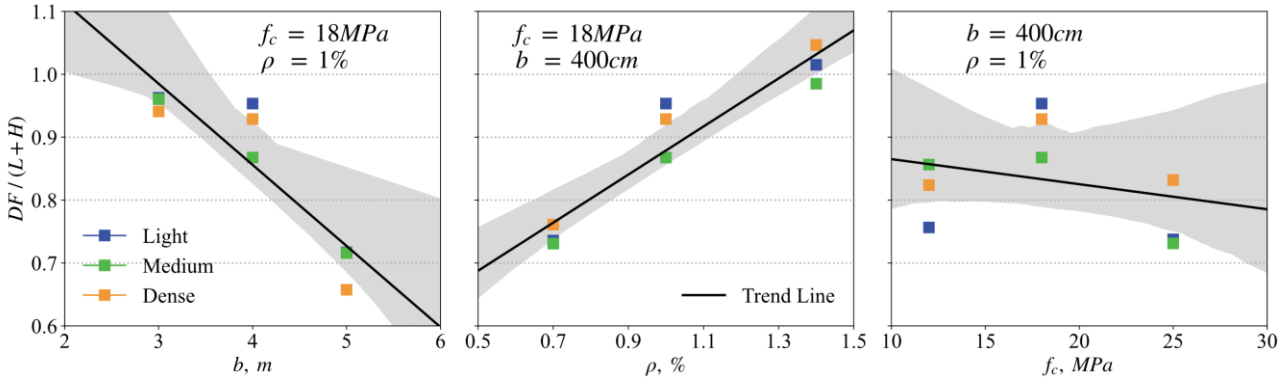

Figure 11. Debris field variations for one-sided collapse with different frame model characteristics, with trend line and 95% confidence interval.

beams collapse near their original positions, forming a relatively high debris pile, reaching up to one and a half stories, rather than spreading horizontally. On the other hand, similar to the normal cases DF length increases with the reinforcement ratio in both beams and columns. The different collapse shapes show that increased longitudinal reinforcement maintains beam continuity during collapse progression, pushing debris further beyond the original building boundaries and increasing CR. In several instances, CR values exceeded those from ordinary the normal removal scenario leading to higher DF values.

6. Conclusions

This study investigated the progressive collapse behavior of reinforced concrete frame structures, focusing on various important factors such as span length, reinforcement ratio, and concrete strength. Extensive numerical analysis based on the Applied Element Method was conducted, leading to several key findings that enhance our understanding of collapse mechanisms and debris field (DF) behavior.

- The analysis revealed a consistent relationship between the debris field length (DF) and the building dimensions. It was found that DF could be reliably calculated as the sum of the total length and height of the building, which provides a reliable estimation for the DF to ensures a minimum safety margin for designing RC building demolition projects.
- The analysis showed that variations in frame properties, such as reinforcement ratio and concrete strength, impact the debris field. However, the effects of transverse reinforcement density were less significant, with overlaps in DF values for different stirrup densities and no significant differences across various spans.
- A comprehensive multi-linear regression analysis was conducted to account for the combined effects of the various building characteristics included in this work. The resulting equation achieved an R^2 value of 0.81, providing a robust equation for predicting DF. And for safety considerations, the equation was conservatively adjusted to account for potential errors, leading to the development of the minimum DF length relation.
- Alternative demolition methods utilizing tension cables were explored to direct the collapse debris to one side, effectively minimizing unintended debris spread. This method reduced DF values compared to the standard approach. The limited impact of stirrup density remained evident in this method also.
- It should be noted that full collapse directed to the inside of the building, where the debris pile stay enclosed within the frame's original boundaries, was investigated but not achieved. Various scenarios for column removal were explored without reaching a complete collapse. Future research should explore alternative strategies and mechanisms to ensure that debris falls within the boundaries of the building, potentially by adding external or internal elements to force the progressive collapse and direct it to the inside area of the building.
- Moreover, the findings of this work are primarily applicable to low-rise, multi-story RC frames with similar structural characteristics and material properties to those numerically modeled, and may not directly extend to other building like high-rise or wall-frame structures without further investigation.

Overall, the findings from this study provide a comprehensive understanding of the factors affecting the progressive collapse of low-rise RC frame structures and the resulting debris field. The proposed equations and methods emphasize the importance and offer practical guidelines for designing safer controlled demolition projects. Also, this work demonstrated the practical applicability of AEM in modeling and analyzing building demolition processes, providing a valuable tool for engineers and researchers in the field of structural engineering.

Acknowledgment

With gratitude and respect, this work was conducted under the supervision and significant contributions of Dr. Mohamed Darweech, who passed away on April 18, 2022. Dr. Darweech was an associate professor and the head of the Structural Engineering Department at Damascus University.

Author contributions

M Nadir Olabi: Conceptualization, Methodology, Investigation, Visualization, Formal analysis, Writing - original draft, Writing -review & editing.

Conflicts of interest

The author declares no conflicts of interest.

References

1. Deringöl, A. H., & Güneyisi, E. M. (2023). Enhancing the seismic performance of high-rise buildings with lead rubber bearing isolators. *Turkish Journal of Engineering*, 7(2), 99-107.
2. Tanyıldızı, M., Karaca, E. O., & Bozkurt, N. (2022). Green concrete production with waste materials as cement substitution: A literature review. *Engineering Applications*, 1(1), 33–45.
3. İLgün, A., Zia, A. J., Sancioğlu, S., Soydoğan, H. F., Köklü, M. H., Aribaş, S., & Bayram, B. (2023). Buckling performance of thin-walled filled steel columns. *Turkish Journal of Engineering*, 7(3), 172–179.
4. Akın, E., & Kanas, E. (2023). Collapse capacity assessment of non-ductile open ground story reinforced concrete frame. *Turkish Journal of Engineering*, 7(2), 157-165.
5. Yılmaz, M., Can, H., & Köktaş, F. (2024). Examination of buildings with different number of floors using non-linear time history analysis according to TBEC-2018 and EC 8 seismic codes. *Advanced Engineering Science*, 4, 76–92.
6. Yuzbasi, J. (2024). Controlled demolition: Novel monitoring and experimental validation of blast-induced full-scale existing high-rise building implosion using numerical finite element

simulations. *Journal of Civil Structural Health Monitoring*.
7. ASCE/SEI7 (Ed.). (2017). Minimum design loads and associated criteria for buildings and other structures. *American Society of Civil Engineers*.
8. Ferraioli, M., Laurenza, B., Lavino, A., & De Matteis, G. (2024). Progressive collapse analysis and retrofit of a steel-RC building considering catenary effect. *Journal of Constructional Steel Research*, 213, 108364.
9. Elkady, N., Augusthus Nelson, L., Weekes, L., Makoond, N., and Buitrago, M. (2024). Progressive collapse: Past, present, future and beyond. *Structures*, 62, 106131.
10. Elsanadedy, H. M., and Abadel, A. A. (2022). High-fidelity FE models for assessing progressive collapse robustness of RC ordinary moment frame (OMF) buildings. *Engineering Failure Analysis*, 136, 106228.
11. Qian, K., Weng, Y.-H., Fu, F., and Deng, X.-F. (2021). Numerical evaluation of the reliability of using single-story substructures to study progressive collapse behaviour of multi-story RC frames. *Journal of Building Engineering*, 33, 101636.
12. Alshaikh, I. M. H., Bakar, B. H. A., Alwesabi, E. A. H., and Akil, H. M. (2020). Experimental investigation of the progressive collapse of reinforced concrete structures: An overview. *Structures*, 25, 881-900.
13. Kiakojouri, F., De Biagi, V., Chiaia, B., and Sheidaii, M. R. (2020). Progressive collapse of framed building structures: Current knowledge and future prospects. Engineering *Structures*, 206, 110061.
14. Kabele, P., Pokorný, T., and Koska, R. (2003). Finite element analysis of building collapse during demolition.
15. Zhang, Q., Zhao, Y.-G., Kolozvari, K., and Xu, L. (2020). Simplified model for assessing progressive collapse resistance of reinforced concrete frames under an interior column loss. *Engineering Structures*, 215, 110688.
16. McKenna, F., Scott, M. H., and Fenves, G. L. (2010). Nonlinear finite-element analysis software architecture using object composition. *Journal of Computing in Civil Engineering*, 24(1), 95-107.
17. Alhafian, S. (2013). Seismic progressive collapse of reinforced concrete frame structures using the Applied Element Method [PhD Dissertation]. Heriot-Watt University.
18. Salvalaggio, M., Bernardo, V., & Lourenço, P. B. (2024). Exploring seismic fragility and strengthening of masonry built heritage in Lisbon (Portugal) via the Applied Element Method. *Engineering Structures*, 320, 118890.
19. Baciu, C., Lupoae, M., Nica, G. B., and Constantin, D. (2019). Experimental and numerical studies of the progressive collapse of a reinforced concrete-framed structure using capacity curves. *Arabian Journal for Science and Engineering*, 44(10), 8805-8818.
20. Cismasiu, C., Ramos, A. P., Moldovan, I. D., Ferreira, D. F., and Filho, J. B. (2017). Applied Element Method simulation of experimental failure modes in RC shear walls. *Computers and Concrete*, 19(4), 365-374.
21. Elshaer, A., Mostafa, H., and Salem, H. (2017). Progressive collapse assessment of multistory reinforced concrete structures subjected to seismic actions. *KSCE Journal of Civil Engineering*, 21(1), 184-194.
22. ELS. (2006). Extreme Loading for Structures Technical Manual (2.4) [Computer software]. Applied Science International.
23. Meguro, K., and Tagel-Din, H. (2000). Applied Element Method for structural analysis: Theory and application for linear materials. *Structural Engineering/Earthquake Engineering*, 17(1), 21s-35s.
24. Tagel-Din, H., and Meguro, K. (2000a). Applied Element Method for simulation of nonlinear materials: Theory and application for RC structures. *Structural Engineering/Earthquake Engineering*, 17(2), 137s-148s.
25. Meguro, K., and Tagel-Din, H. (2001). Applied element simulation of RC structures under cyclic loading. *Journal of Structural Engineering*, 127(11), 1295-1305.
26. Meguro, K., and Tagel-Din, H. S. (2002). Applied Element Method used for large displacement structural analysis. *Journal of Natural Disaster Science*, 24(1), 25–34.
27. Tagel-Din, H., and Meguro, K. (2000b). Applied Element Method for dynamic large deformation analysis of structures. *Structural Engineering/Earthquake Engineering*, 17(2), 1(215s)-10(224s).
28. Tagel-Din, H., and Meguro, K. (2000c). Analysis of a small-scale RC building subjected to shaking table tests using Applied Element Method. *12th World Conference on Earthquake Engineering*.
29. Sasani, M. (2008). Response of a reinforced concrete infilled-frame structure to removal of two adjacent columns. *Engineering Structures*, 30(9), 2478–2491.
30. Griffin, J. W. (2008). Experimental and analytical investigation of progressive collapse through demolition scenarios and computer modeling [Master Thesis]. North Carolina State University.
31. Lupoae, M., and Bucur, C. (2009). Use of applied element method to simulate the collapse of a building. SISOM 2009 and Session of the Commission of Acoustics, 13–18.
32. Muto, K. (1965). Strength and deformations of structures. *Maruzen Co. Ltd*.
33. Okamura, H., and Maekawa, K. (1991). Nonlinear analysis and constitutive models of reinforced concrete. *Gihodo Co. Ltd*.
34. Ristic, D., Yamada, Y., and Iemura, H. (1986). Stress-strain based modeling of hysteretic structures under earthquake induced bending and varying axial loads (Reseach Report 86-ST-01). *School of Civil Engineering, Kyoto University*.
35. Syrian Code. (1995). Arabic Syrian Code for Design and Execution of Reinforced Building Structures. *Syrian Engineers Union*.
36. Olabi, M. N. (2012). Practical analysis to remove multi-story low-rise building by modeling using Applied Element Method [Master thesis]. Damascsus University.

Appendix A

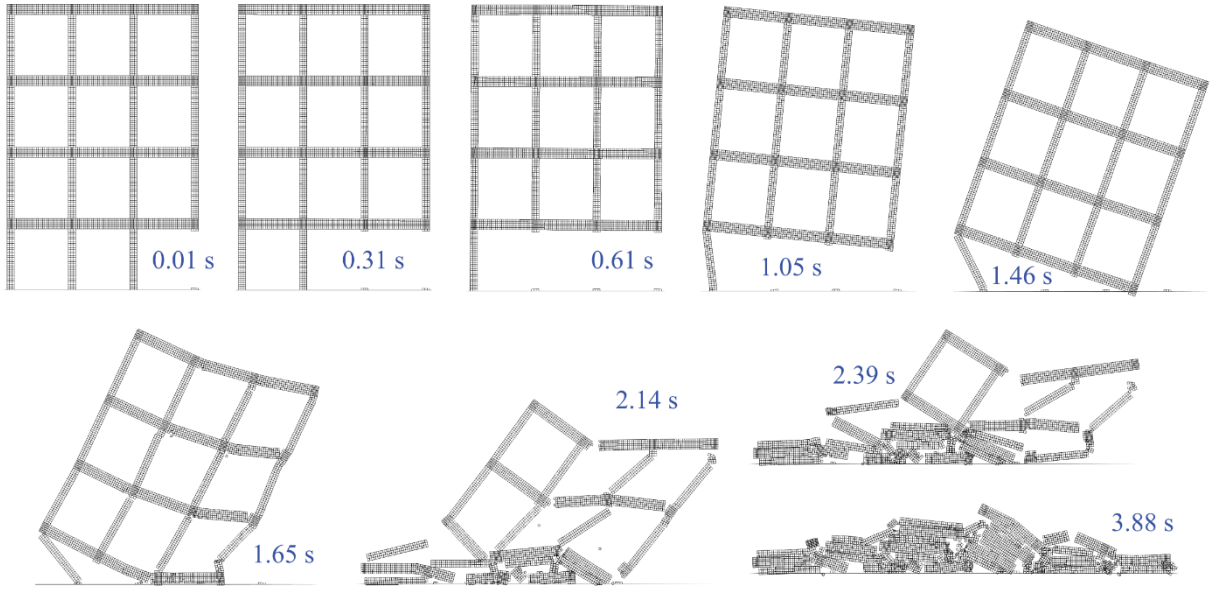

Figure A1. Mechanism and progressive collapse form for frame E5

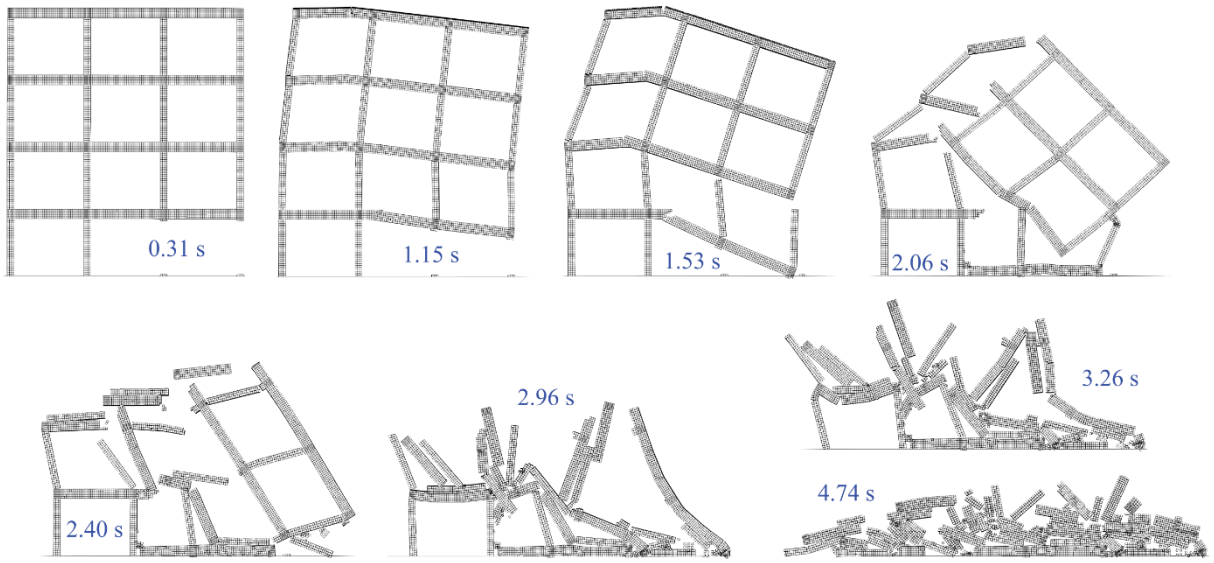

Figure A2. Mechanism and progressive collapse form for frame E10

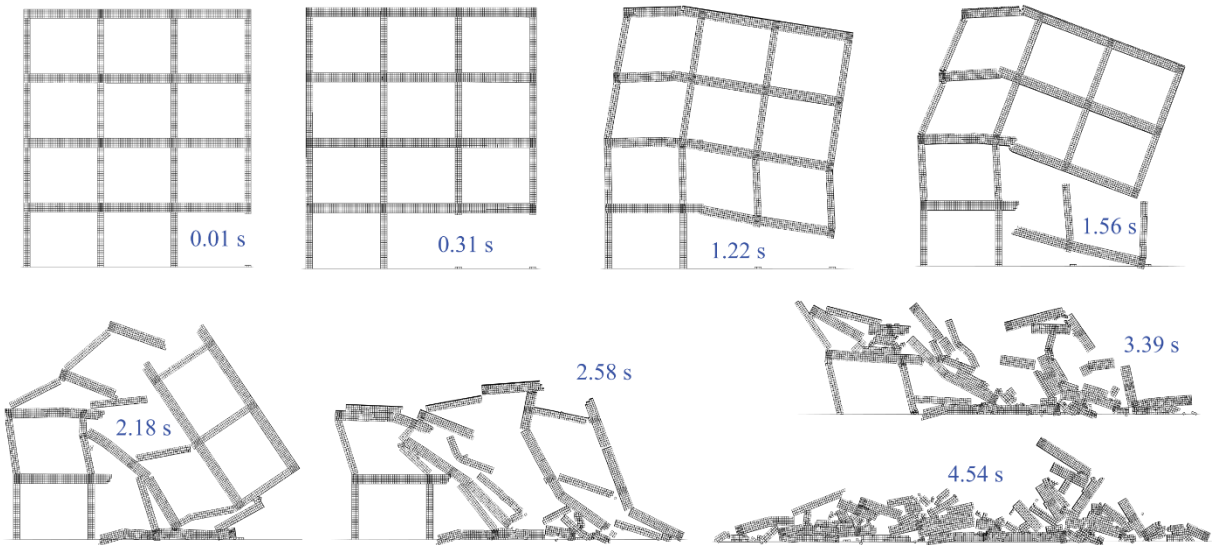

Figure A3. Mechanism and progressive collapse form for frame E17

Appendix B

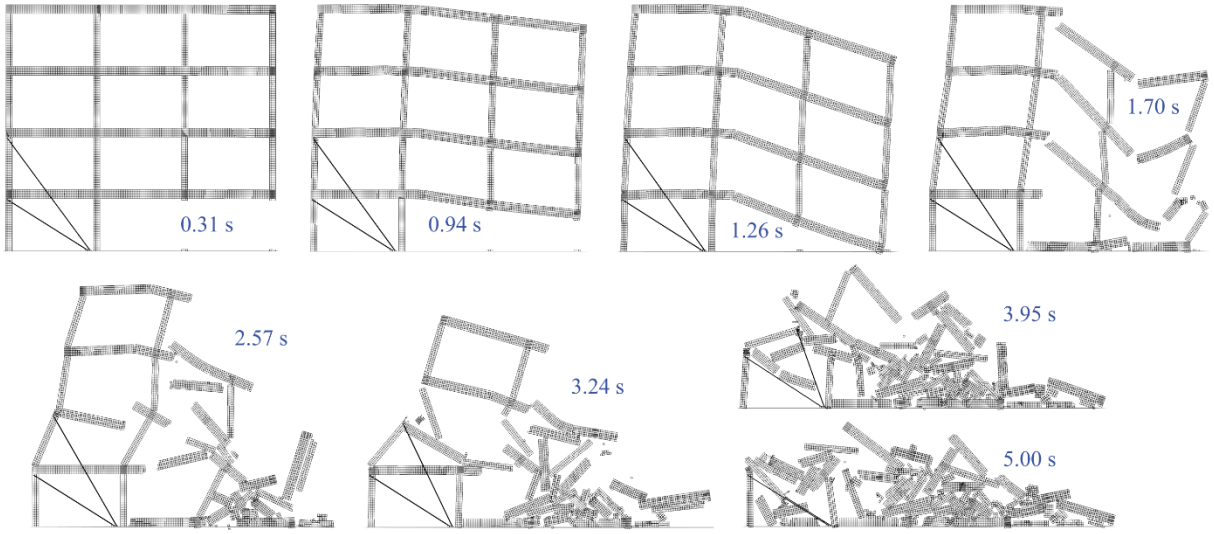

Figure B1. Mechanism and progressive collapse form for one-sided collapse scenario, frame E8

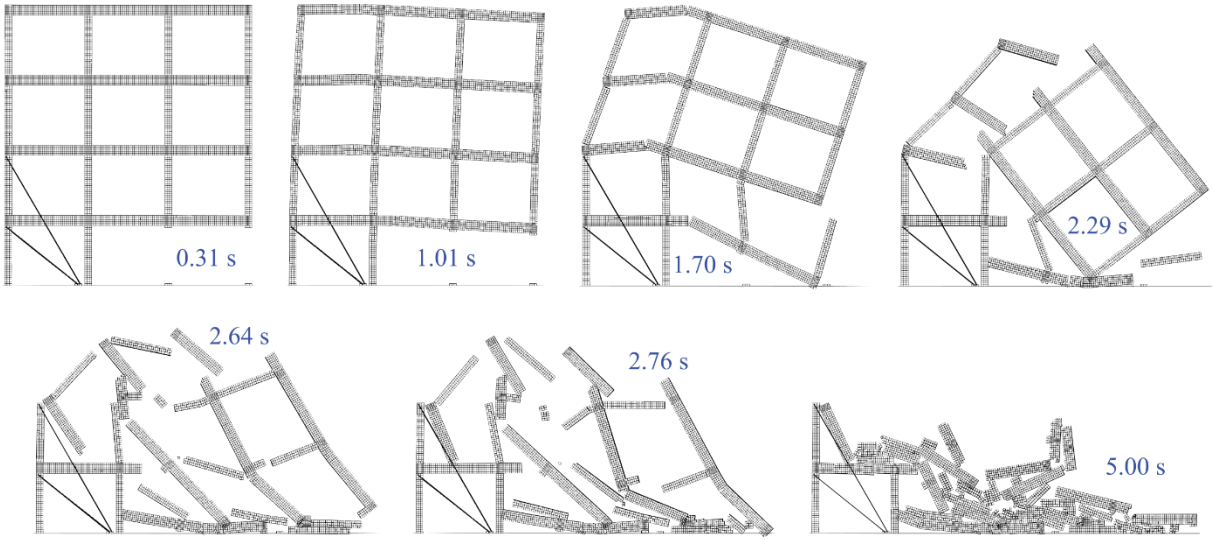

Figure B2. Mechanism and progressive collapse form for one-sided collapse scenario, frame E20